

Article

Planifilum fulgidum Is the Dominant Functional Microorganism in Compost Containing Spent Mushroom Substrate

Hong Zhang ¹, Wenying Wang ², Zaixue Li ³, Chuanlun Yang ³, Shuang Liang ⁴ and Lushan Wang ^{1,*}

¹ State Key Laboratory of Microbial Technology, Shandong University, Qingdao 266237, China; 201712288@mail.sdu.edu.cn

² School of Life Sciences, Qinghai Normal University, Xining 810016, China; wenyingwang@qhnu.edu.cn

³ Shandong Chambroad Holding Group Co., Ltd., Boxing 256599, China; zaixuelove@126.com (Z.L.); yang@163.com (C.Y.)

⁴ School of Environmental Science and Engineering, Shandong University, Qingdao 266237, China; liangshuang@sdu.edu.cn

* Correspondence: lswang@sdu.edu.cn

Abstract: The extensive accumulation of spent mushroom substrate (SMS) owing to the large-scale production of edible fungi is causing environmental problems that cannot be ignored. Co-composting is a promising method for agricultural and animal husbandry waste disposal. In this study, the composition and function of microbial communities in the process of cattle manure–maize straw composting with SMS addition were compared through an integrated meta-omics approach. The results showed that irrespective of SMS addition, the predominant fungi were Ascomycota, while the dominant bacteria were Firmicutes, Proteobacteria, Actinobacteria, and Bacteroidetes. High temperature promoted the evolution from Gram-negative bacteria (Bacteroides, Proteobacteria) to Gram-positive bacteria (Firmicutes, Actinomycetes). The composting process was accelerated by SMS addition, and the substrate was effectively degraded in 14 days. Metaproteomics results showed that the dominant microorganism, *Planifilum fulgidum*, secreted large amounts of S8, M17, and M32 proteases that could degrade macromolecular protein substrates in the presence of SMS. *Planifilum fulgidum*, along with *Thermobifida fusca* and *Melanocarpus albomyces*, synergistically degraded hemicellulose, cellulose, and protein. In addition, the dominant microorganisms related to the initial raw materials such as *Pichia*, *Lactobacillus* in the microbial agent and *Hypsizygus* in SMS could not adapt to the high-temperature environment (>60 °C) and were replaced by thermophilic bacteria after 5 days of composting.



Citation: Zhang, H.; Wang, W.; Li, Z.; Yang, C.; Liang, S.; Wang, L. *Planifilum fulgidum* Is the Dominant Functional Microorganism in Compost Containing Spent Mushroom Substrate. *Sustainability* **2021**, *13*, 10002. <https://doi.org/10.3390/su131810002>

Academic Editor: Chunjiang An

Received: 10 July 2021

Accepted: 3 September 2021

Published: 7 September 2021

Publisher's Note: MDPI stays neutral with regard to jurisdictional claims in published maps and institutional affiliations.



Copyright: © 2021 by the authors. Licensee MDPI, Basel, Switzerland. This article is an open access article distributed under the terms and conditions of the Creative Commons Attribution (CC BY) license (<https://creativecommons.org/licenses/by/4.0/>).

Keywords: co-composting; microbial agent; microbial diversity; metaproteomics; *Planifilum*

1. Introduction

Spent mushroom substrate (SMS) is a solid culture material discarded after the harvest of edible fungi. In general, the raw materials used for the cultivation of edible fungi include agricultural and forestry wastes, such as corn cob, cottonseed shell, wood chips, and other nutrition-rich organic matter [1]. It is estimated that more than 13 million tons of SMS are generated in China each year, causing environmental problems that cannot be ignored [2–4]. SMS contains numerous mycelia and edible fungal metabolites, such as carbohydrates, proteins, organic acids, and bioactive substances, which have the potential of ecological high-value utilization [5,6]. In addition, with large-scale planting and intensive breeding, the substantial increase in straw and livestock manure has become a major problem for the sustainable development of agriculture and ecological environmental protection in China [7,8]. Reasonable use of these wastes can improve the economic benefits, protect the environment, and accomplish recycling of wastes and sustainable development of agriculture.

Aerobic composting is considered as an efficient and sustainable technology for organic wastes disposal, because it limits the overall environmental pollution, and its end product is suitable for use as a fertilizer and soil amendment [9,10]. Co-composting uses a combination of different organic wastes and appropriate parameters to provide ideal conditions for the composting process [11]. This approach can not only treat different organic wastes simultaneously but it also can make comprehensive use of different waste properties, shorten the fermentation period, and improve the quality of compost [12,13]. In a previous study, Zhang et al. [14] confirmed the rationality of co-composting with straw and cow dung. The high temperature generated by the accumulation of microbial metabolism can effectively kill harmful mesophilic organisms, such as *Acinetobacter*, *Pseudomonas*, and nematodes. Meanwhile, the dominant microflora (Firmicutes, Actinomycetes) in the composts was beneficial to crop plants in eliminating pathogens (through the release of some antibiotics) and environmental stress tolerance (through the secretion of signal compounds) [15,16]. The antifungal and protease activities of dominant composting bacteria *Bacillus* can reduce the infection rate of bacterial wilt and other fungal diseases of tomatoes and cucumbers [17]. In order to maintain the beneficial microorganisms, tomato root could exude lactic acid and hexanoic acid to favor the growth of *Bacillus cereus* [18].

Composting is a process in which a variety of microorganisms participate in the degradation and transformation of organic matter. Owing to the complexity of co-composting substrates, the composting process is mainly dependent on the interaction of microorganisms and their secreted degradative enzyme systems [14]. With the development of genomics technology, the dominant microbial community and its dynamics in the process of high-temperature aerobic composting with various substrates have been examined [19–21]. By using metaproteomic methods, the dominant microorganisms and their functional enzymes involved in the degradation of organic matter can be located and identified [22]. Integrated “omics” approaches enable linking the microbial community structure to function, and they elucidate the degradation mechanism of lignocellulosic composting.

With the advancement in microbial technology, more and more microbial agents are widely used in practical application to improve composting. Previous studies have indicated that the addition of single or mixed microbial agents can increase the temperature of thermophilic stage during composting as well as prolong the thermophilic stage [8,23,24]. Wei et al. [25] reported that the inoculation of thermophilic actinomycetes increased the cellulase activity and promoted lignocellulosic degradation. Furthermore, the addition of functional bacteria has been observed to accelerate nitrogen conversion and decrease ammonia–nitrogen emissions, thus reducing nitrogen loss [26–28]. However, some studies have shown that the addition of inoculants had no significant effect on shortening the composting duration [29]. Ballardo et al. [30] observed that the presence of *Bacillus thuringiensis* did not alter the global structure of the dominant microbial community associated with the final product and did not affect its potential use as a fertilizer. Thus, the mechanism of the effect of microbial agent addition on the composting process and microbial community is still unclear.

In the present study, two composting processes with and without SMS addition were performed in parallel to evaluate the effects of changes in the substrate on the structure and function of microorganisms. Concurrently, to investigate the role of microbial agents in the composting process, groups of microbial agents were added to the composting processes. By using 16S rRNA and ITS rRNA high-throughput sequencing, the composition and dynamic changes of microbial communities in bacteria and fungi during the composting process were monitored, and a metaproteomic approach was employed to directly observe the functions of the dominant communities during the composting process. The results of this study provided novel insights into the degradation mechanism of co-composting and practical application of microbial agents.

2. Materials and Methods

2.1. Materials and Compost Sampling

The composting process was conducted at Shandong Bohua High-efficient Ecological Agriculture Science & Technology Co., Ltd., Binzhou, Shandong Province, China (37°21' N, 118°26' E, measured by ASHTECHGPSZ-X). Aerobic composting started on 6 January 2019 and lasted for 29 days. The experimental materials were collected from the surrounding cow farms and mushroom factories. The microbial agent was purchased from Shandong Chambroad Holding Group Co., Ltd., China, and high-throughput sequencing revealed that the inoculum was a combination of three genera: *Acetobacter*, *Lactobacillus*, and *Pichia*. The four composting systems were (1) Corn straw and cow dung mixed at a mass ratio of 1:2 (SC); (2) Corn straw and cow dung mixture (mass ratio of 1:2) inoculated with 0.3% microbial inoculum (SCI), (3) Corn straw, cow dung, and SMS mixed at a mass ratio of 1:2:2 (SCM), and (4) Corn straw, cow dung, and SMS mixture (mass ratio of 1:2:2) inoculated with 0.3% microbial inoculum (SCMI). Each compost was piled up outside in a strip (6 m × 2.5 m × 1.5 m).

Samples were collected from a depth of 30–40 cm because the middle layer is considered to be the most suitable for microbial growth [31]. For each pile, three subsamples weighing approximately 0.5 kg were randomly collected from three different positions on days 0, 1, 2, 5, 7, 14, 21, and 29. A total of 96 samples were collected from different compost piles at various times. Each sample was separated into two parts, with one part used for physicochemical analysis and the other part frozen at −80 °C for DNA extraction and protein analysis.

2.2. Analysis of Physicochemical Properties

The temperature of each sampling point was measured with a thermometer (TES1310, TES, Taiwan, China) at each sampling time. To assess the moisture content, the samples were oven-dried at 105 °C until it reached a constant weight. Fresh samples were mechanically shaken with distilled water at a ratio of 1:9 (*w/v*) at 4 °C overnight. The pH and electrical conductivity (EC) of the aqueous extract were measured using a pH meter (FiveEasy Plus FE28, METTLER TOLEDO, Shanghai, China) and conductivity meter (DDSJ-308A, INESA, Shanghai, China), respectively. All the above-mentioned parameters were evaluated in triplicate, and the final results were the average of the three measurements. The total organic carbon (TOC) content was ascertained by the Walkley–Black dichromate oxidation procedure [32], and total nitrogen (TN) content was determined by using the Kjeldahl method [33].

2.3. Enzyme Activity Assay

Each sample was mixed with distilled water at a ratio of 1:9 (*w/v*) at 4 °C overnight, filtered, and centrifuged at 8000 × *g* for 10 min at 4 °C. The supernatant containing crude enzymes was collected and subjected to enzymes (cellulase and xylanase) activities assay and native polyacrylamide gel electrophoresis (PAGE). The activities of xylanase and cellulase were determined by using the 3,5-dinitrosalicylic acid (DNS) method with a multifunctional microporous plate detector (Infinite M200 Pro, TECAN, Shanghai, China) as described previously in Xing et al. [34] with some modifications, and the supernatant of 1% xylan (1% carboxymethylcellulose) dissolved in Na₂HPO₄-citric acid buffer (pH 5.5) was used as substrate.

Native PAGE was performed according to the method described by Zhang et al. [35]. After electrophoresis, the gel was first incubated in carboxymethylcellulose solution (substrate of cellulase) or 2% xylan solution (substrate of xylanase) at 60 °C for 30 min and then de-stained with 1M NaCl solution following its staining in Congo red solution for 10–20 min. Finally, the gel images were visualized using a scanner (CanoScan 9000F, Canon, Beijing, China).

Gelatin zymography was performed as described by Tsujii et al. [36] with modifications, as follows: crude enzymes were separated on 12.5% SDS-PAGE with 1 mg/mL

gelatin incorporated into the gel mixture. After electrophoresis, the gel was first washed twice with 2.5% Triton X-100 to remove SDS, rinsed twice with 2.5% Triton X-100/0.6% Tris, and finally transferred to 0.6% Tris (pH 8.0) and incubated at 60 °C for 1.5 h following washed two times. Subsequently, the gel was stained with 0.5% Coomassie Blue for 1 h, de-stained with 10% acetic acid/10% ethanol, and visualized using a scanner (CanoScan 9000F, Canon, Beijing, China).

2.4. DNA Extraction and Amplicon Sequencing

The total DNA was extracted from each sample collected on days 1, 5, 14, and 29 using E.Z.N.A.[®] soil DNA Kit (Omega Bio-tek, Norcross, GA, USA) according to the manufacturer's protocols. The representative DNA sample was a mixture of three subsamples extracted from 0.5 g of each experimental sample. The final DNA concentration and purification were determined using a NanoDrop 2000 spectrophotometer (Thermo Scientific, Wilmington, NC, USA), and the DNA quality was verified by 1% agarose gel electrophoresis. The extracted DNA was used for pyrosequencing on a MiSeq platform (Shanghai Majorbio Technology, China). In brief, the V3–V4 hypervariable regions of the bacterial 16S rRNA gene were amplified with primers 338F (5'-ACTCCTACGGGAGGCAGCAG-3') and 806R (5'-GGACTACHVGGGTWICTAAT-3'), while the internal transcribed spacers (ITS) rRNA amplification for fungal diversity was performed with the barcoded fusion primers ITS1 (5'-TCCGTAGGTGAACCTGCGG-3') and ITS4 (5'-TCCTCCGCTTATTGATATGC-3'). The PCR amplification was performed as follows: initial denaturation at 95 °C for 3 min, followed by 30 cycles of denaturation at 95 °C for 30 s, annealing at 55 °C for 30 s, and elongation at 72 °C for 45 s, a final extension at 72 °C for 10 min, and termination of the reaction at 4 °C. The PCR products were extracted using 2% agarose gel electrophoresis and further purified by employing AxyPrep DNA Gel Extraction Kit (Axygen Biosciences, Union City, CA, USA). The purified amplicons were pooled in equimolar amounts and paired-end sequenced on an Illumina MiSeq platform (Illumina, San Diego, CA, USA) according to the standard protocols developed by Majorbio Bio-Pharm Technology Co. Ltd. (Shanghai, China).

The raw data were demultiplexed, quality-filtered, and merged using FLASH [37]. Operational taxonomic units (OTUs) with 97% similarity cutoff were clustered using UPARSE version 7.1 (<http://drive5.com/uparse/> (accessed on 28 July 2019)), and chimeric OTUs were identified and removed using the UCHIME method [38]. The taxonomy of clustered OTUs was analyzed by Ribosomal Database Project (RDP) Classifier version 2.2 [39] against the 16S rRNA database (<http://www.arb-silva.de> (accessed on 10 September 2019)) and ITS database (<http://unite.ut.ee/index.php> (accessed on 10 September 2019)) using a confidence threshold of 0.7.

2.5. Metaproteomics and Bioinformatics Analyses

Proteins were extracted from each sample collected on days 1 and 14 as described by [40]. In brief, 100 g of a mixture of three subsamples were soaked in 400 mL of water and shaken overnight at 4 °C. After centrifugation, the supernatant was collected and ultrafiltered using a 3 kDa cutoff membrane (Sigma-Aldrich, Burlington, MA, USA). After precipitation with trichloroacetic acid and resuspension in double-distilled water, the concentration of proteins was determined using the method developed by [41]. Subsequently, 50 µg of proteins from each sample were denatured by mixing with 50 µL of degeneration buffer and reduced by incubation with 30 µL of dithiothreitol (1 M) for 2 h at 37 °C. Then, 50 µL of iodoacetamide (1 M) were added to the mixture and placed in dark for 1 h for alkylation. The proteins were digested with trypsin (1:50 *w/w*, trypsin/centrifuged proteins) and stirred overnight at 37 °C. After desalination with Millipore ZipTip C18 column (Sigma-Aldrich), the peptides were dissolved in 10 µL of elution buffer containing 50% (*v/v*) acetonitrile and 0.1% (*v/v*) trifluoroacetic acid. Subsequently, the peptides were analyzed by liquid chromatography-tandem mass spectrometry (LC-MS/MS) at Shandong

University, with a Prominence nano LC system (Shimadzu) coupled to an LTQ-Orbitrap Velos Pro ETD mass spectrometer (Thermo Fisher Scientific, Shanghai, China).

Raw data were analyzed using Proteome Discoverer software 1.4 (Thermo Fisher Scientific) with a SEQUEST search engine. The genera with relative abundances >2% (including 7 dominant fungal genera and 21 dominant bacterial genera) were used as references. Oxidation was set as dynamic modification, and carbamido methylation was considered as static modification. Automatic decoy database searches were used to filter the search results with a false discovery rate of 0.05. Protein identification was approved only when the probability reached <0.05 and at least two peptides were identified (q -value < 0.05). A protein was considered effective when it was recognized in at least two replicates. Signal peptide sequences were classified using SignalP 4.1.

2.6. Statistical Analysis

Analysis of the physicochemical properties was performed using GraphPad Prism (version 7.0). The microbial diversity data were examined using the free online platform of Majorbio I-Sanger Cloud Platform (www.i-sanger.com (accessed on 20 October 2019)). A co-occurrence network of bacterial and fungal community was conducted by calculating the Spearman correlation coefficients using the relative abundance of OTUs ($r > 0.8$, $p < 0.05$) which were detected in at least 5 samples and had sum reads >0.5% based on R (Version 4.0.2) package 'Hmisc'. The enzymes spectra were constructed using Photoshop Version 3.0, and heatmap and histograms of metaproteomics were derived using MATLAB (version R2014a).

3. Results and Discussion

3.1. Physicochemical Properties of the Four Composting Systems

Temperature is known to be a critical parameter for accomplishing composting, and the four piles examined in the present study maintained high temperature (>60 °C) for more than 3–5 days (Figure 1a), which could eliminate weed seeds and pathogens and meet the requirements of environmental hygiene [42]. All of the four compost piles maintained the composting temperature at >50 °C for more than 2 weeks. The highest temperature was noted on day 2 in SCI and SCM but on day 4 in SC and SCMI. Unlike a fermenter, high temperature could not be maintained continuously in the present study, owing to the implementation of open strip composting conducted outdoors in winter [22], and there was no significant difference in temperature among SC, SCI, SCM, and SCMI (one-way ANOVA, $p < 0.05$). These results indicated that the addition of microbial agents did not promote the early onset of thermophilic phase, which is consistent with the finding reported by [43], that commercial microbial inoculants do not have significant effects on the thermophilic stage of composting, unlike other microbial inoculants that extend or shorten the compost heating stage [23,44]. The composting process ceased when the temperature dropped to about 20 °C on day 29.

To ensure successful composting, the initial moisture contents of the four compost piles were adjusted to 50–58% (Figure 1b). However, with the increase in microbial metabolism and evaporation, the moisture content of each pile showed a gradual decline. The final moisture contents of SCM and SCMI were 5–10% lower than those of SC and SCI, indicating that the fluffy texture of SMS with good air permeability increased moisture volatilization during composting. Similar conclusions have also been reported by Li et al. [45], who found that the addition of an appropriate proportion of SMS as a bulking agent shortened the fermentation duration by increasing gas exchange and accelerating the drying speed of the material.

The pH and EC of all the four composting systems generally increased with time (Figure 1c,d), which is consistent with the results noted in natural corn stalk composting [14]. SMS addition lowered the pH of the composting system (one-way ANOVA, $p < 0.01$), which is similar to that observed with the addition of SMS to garden waste [46]. The lowest pH detected on day 5 was owing to the rapid degradation of readily available organic matter

and accumulation of organic acids [47], while the subsequent gradual increase in pH may be owing to the degradation of protein substances and accumulation of ammonium [48]. The pH values of the four composting systems were within an acceptable range of 7–9 [49]. The final EC of the four composting systems did not exceed 4 mS/cm, which is considered as an upper threshold for plants with medium salinity sensitivity [50].

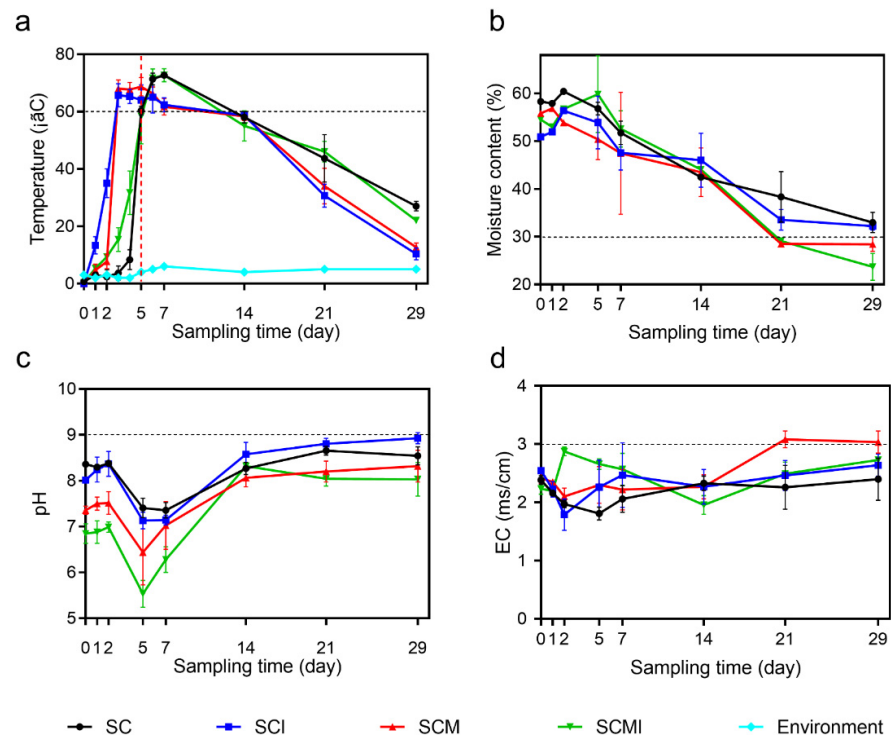


Figure 1. Changes in the physicochemical parameters during composting. Temperature (a), moisture (b), pH (c), and EC (d) of the four composting systems.

3.2. Characterization of the Microbial Communities

The ITS and 16S amplicon diversity sequencing was performed using samples collected on days 1, 5, 14, and 29 from the four composting systems. A total of 1,000,480 and 1,004,779 ITS and 16S rDNA sequences were obtained, which clustered into 862 and 2315 ITS and 16S OTUs according to 97% sequences similarity, respectively. Table 1 shows the OTUs determined in each sample. The number of OTUs in the four composting systems decreased with composting time, indicating that high temperature, as the key environmental selection pressure for composting, could effectively reduce the diversity of microorganisms. The number of bacterial OTUs slightly increased when the ambient temperature dropped to about 20 °C on day 29 and the high-temperature screening environment was removed [51]. Likewise, the Chao1 index, which represents community richness, showed the same trend as OTUs, implying that a simple and stable community structure was formed during the composting process, and the bacterial community diversity was always higher than that fungal community diversity.

The Shannon index represents community diversity, and a higher value denotes higher community diversity [26]. The bacterial community diversity in SCM was significantly lower than that in SC (Chao1 index, $p < 0.05$), indicating that the addition of raw materials such as SMS reduced the bacterial community diversity (Figure 2e). Non-metric multidimensional scaling (NMDS) analysis revealed that the microbial communities were well clustered in the four composting systems (Figure 2b,f). Similarity analysis showed that the bacterial and fungal communities were homogenous across the four composting systems (Figure 2c,g, Bray–Curtis analysis, $p > 0.05$), suggesting a high similarity in bacterial and fungal community composition among the four systems, similar to that reported by [52].

Overall, 222 ITS and 706 16S OTUs were shared among the four composting systems, respectively, with a higher number of unique OTUs detected in SC and SCI (Figure 2d,h).

Table 1. Overview of sequencing data.

pile	Time	Fungi			Bacteria		
		Seq-num	OTUs	Chao1	Seq-num	OTUs	Chao1
SC	1 d	71,756	448	517	50,990	1653	1808
	5 d	58,897	432	437	55,303	742	1119
	14 d	60,693	269	286	46,654	660	905
	29 d	61,284	147	155	52,092	943	1097
SCI	1 d	73,566	430	425	61,831	659	856
	5 d	74,619	375	385	56,385	750	995
	14 d	74,243	274	284	59,454	584	647
	29 d	74,055	222	217	71,910	801	883
SCM	1 d	34,452	245	289	72,962	584	893
	5 d	64,908	341	385	63,189	1222	1493
	14 d	43,927	149	170	54,033	379	522
	29 d	57,564	89	115	71,100	540	696
SCMI	1 d	34,607	203	205	71,239	777	907
	5 d	74,430	352	397	70,632	1552	1798
	14 d	71,465	97	94	73,948	309	375
	29 d	70,014	17	12	73,057	327	417
Total		1,000,480	4090	—	1,004,779	12,482	—

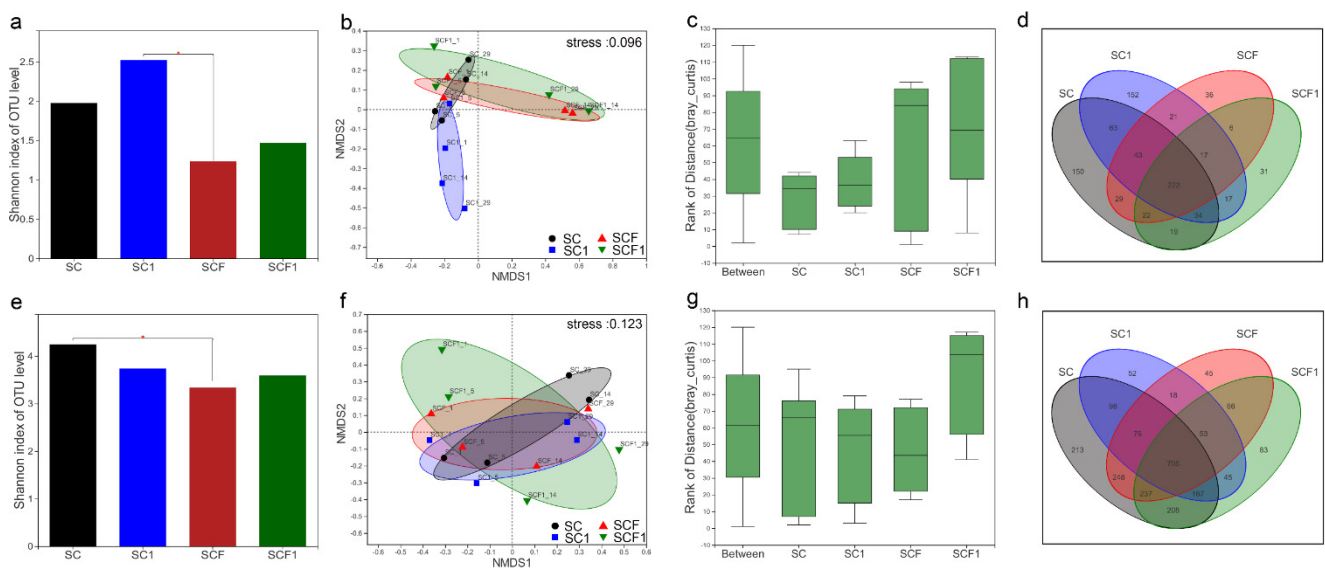


Figure 2. Overview of the microbial diversity of the four composting systems. Shannon index reflected the fungal (a) and bacterial (e) community diversity among the four systems. NMDS analysis showed four clustering patterns of fungi (b) and bacteria (f). ANOSIM analysis based on Bray–Curtis distances calculated at OTU level revealed similar fungal (c) and bacterial (g) composition in the four composting systems. Venn diagram indicated the shared and unique OTUs of fungi (d) and bacteria (h) in the four composting systems.

3.3. Composition of the Fungal Communities

The fungal communities were relatively simple and stable at the phylum level in all the four composting systems. A total of 11 fungal phyla were identified in 16 samples, among which Ascomycota and Basidiomycota were predominant, accounting for nearly 98% of all the sequences (Figure 3a). Ascomycetes, which can utilize a variety of carbon sources and adapt well to high-temperature pressure and nutritional deficiency, were the most abundant in the composting systems [53]. Owing to their ability to secrete cellulase and

hemicellulase, Ascomycota had been reported to be the dominant phylum in lignocellulosic compost ecosystems [54]. As mushrooms belong to Basidiomycota, SMS addition increased the initial Basidiomycota content in SCM and SCMI when compared with that in SC and SCI. However, with the increasing composting time to the 5th day, the Basidiomycota content in SCM and SCMI significantly decreased, while Ascomycota became dominant in all the four composting systems, accounting for >99% of the fungal sequences. This finding indicated that Ascomycota plays a dominant role in lignocellulosic composting [14].

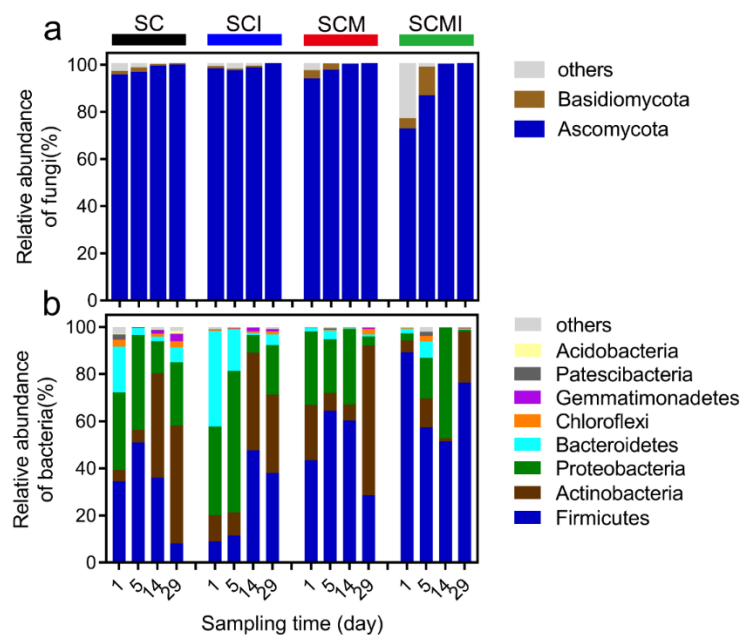


Figure 3. Compositions of fungal (a) and bacterial (b) communities at the phylum level.

The top 20 fungal genera with relatively high abundance clustered into four branches (a–d), and the abundances of genera in branches a and b gradually decreased with the composting time, while those of genera in branches c and d remained high throughout the composting process (Figure 4a). On days 1–5, *Thermomyces* and *Aspergillus* in branch d were dominant in the four composting systems, with an average relative abundance over 36%; in contrast, the average relative abundance of other fungi such as *Candida*, *Penicillium*, *Talaromyces*, *Pseudallescheria*, and *Mycothermus* in branches a, b, and c was <7%. In particular, *Hypsizygus* from SMS was detected in SCM and SCMI on days 1 and 5, while *Pichia* from the microbial agent was found only in SCMI on day 1. With the onset of the thermophilic stage, the composition of the fungal community significantly changed. In SC and SCI, the relative abundance of fungi in branches a and b decreased, although some fungi could still be detected on days 14 or 29. In contrast, in SCM and SCMI, the relative abundance of fungi in branches a and b was almost undetectable on day 14. These results indicated that non-composting native fungi could not adapt to the high-temperature composting environment and were replaced by thermophiles, and that SMS addition promoted the succession of microbial communities. It must be noted that *Pichia* is highly active in degrading organic acids at low temperature but not at high temperature [55].

The addition of SMS significantly reduced the initial content of fungi in branch c but increased that of fungi in branch a, implying that the amendment of raw materials mixture could change the initial microbial content but could not alter the trend of microbial community succession. Furthermore, during the thermophilic stage, *Thermomyces* and *Aspergillus* (branch d) were dominant in SC and SCI, whereas *Melanocarpus* became dominant in the middle and late stages in SCM and SCMI, with a relative abundance of >85% on day 14. *Thermomyces* is known to secrete large amounts of xylanase and is a key lignocellulose-degrading fungus in lignocellulosic composting [56], cow manure

composting [57], and reed manure composting [51]. *Aspergillus* can adapt to changes in temperature and humidity, and it can produce cellulase and hemicellulase to promote compost maturity [58,59]. *Melanocarpus* belongs to the family Chaetomiaceae, and it can secrete cellulase, xylanase, and laccase [60]. In the present study, significant differences in fungal community composition were found among the four composting systems (Figure S1), with SC and SCM exhibiting significant variation in the abundance of *Mycothermus* (maximum abundance of 12.8%) and *Myceliophthora* (maximum abundance of 5%) (Kruskal–Wallis H test, $p < 0.05$). These results indicated that the addition of SMS had a substantial effect on the composition of the fungal community in the composting systems, and that the fungal community had weak adaptability to environmental changes, such as raw materials, which is consistent with the results of Li et al. [61].

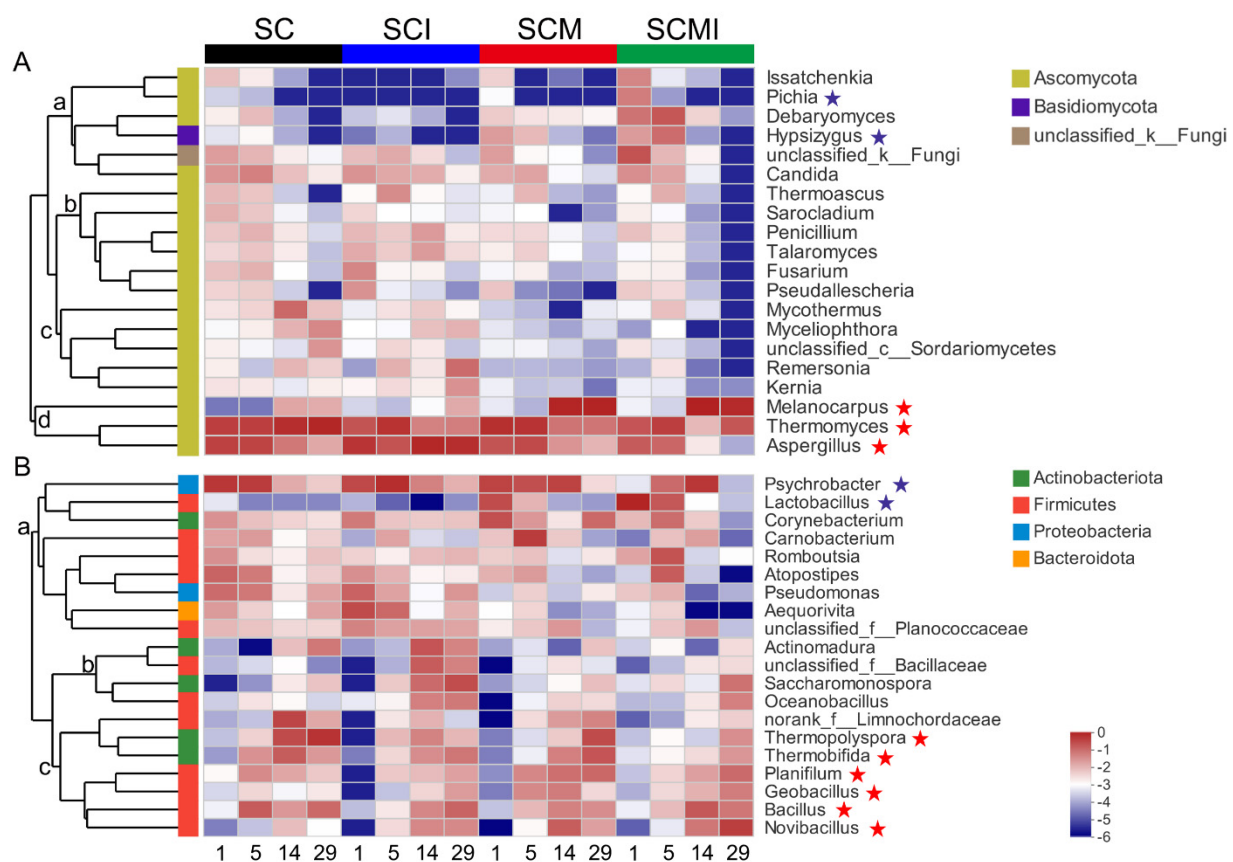


Figure 4. Community heatmap analysis of the top 20 most abundant fungi (A) and bacteria (B) at the genus level. The genera marked with navy blue stars represent bacteria that decreased with an increase in fermentation time, and the red stars represent bacteria that increased with an increase in fermentation time.

3.4. Composition of the Bacterial Communities

Through taxonomic analyses of the 16S rRNA sequences, a total of 35 bacterial phyla were identified. Firmicutes, Proteobacteria, Actinobacteria, and Bacteroidetes were the dominant bacterial phyla in the four composting systems, accounting for nearly 98% of all the sequences. Similar findings have also been noted previously in agricultural and animal husbandry waste composting [52,62]. The abundance of Firmicutes was significantly different among the four composting systems (Figure S2, Kruskal–Wallis H test, $p < 0.05$), whereas that of Proteobacteria, Actinobacteria, and Bacteroidetes did not exhibit significant differences among the four composting systems (Kruskal–Wallis H test, $p > 0.05$). Firmicutes usually prioritize the use of readily degradable organics, such as proteins, fats, and soluble sugars, before being replaced by Actinomycetes that efficiently degrade lignocellulose [51]. The abundance of Firmicutes in SCM and SCMI was significantly higher than that in

SC and SCI (Figure 3B), which could be owing to the high content of carbohydrates, proteins, and fats in SMS [46]. On day 29, the relative abundance of Gram-positive bacteria (including Firmicutes and Actinomycetes) in SCM and SCMI was >92%, which was much higher than that noted in SC and SCI (average 65%), suggesting that the addition of high-nitrogen-containing SMS promoted the evolution of Gram-positive bacteria. In all the four composting systems, the abundances of Proteobacteria and Bacteroidetes decreased, while that of Actinobacteria increased with time, which was consistent with the results of lignocellulose-based manure composting and was not affected by the addition of SMS and microbial agents. In SC and SCI, the abundance of Bacteroidetes was significantly higher than that in SCM and SCMI, implying that the addition of SMS could reduce the initial abundance of Bacteroidetes. Bacteroidetes, which are not high-temperature-tolerant and decrease in abundance with composting time, are not the core bacteria that produce lignocellulose hydrolases [20].

To explain the role of bacterial activity in the composting systems, the bacterial abundance was analyzed at the genus level (Figure 4B). In all of the four composting systems, the predominant bacterial genera in the initial stage of composting belonged to branch a, and they mainly included *Psychrobacter* (average relative abundance of 22% on days 1–5) and *Pseudomonas* of Proteobacteria, *Corynebacterium* of Actinobacteria, *Carnobacterium*, *Romboutsia*, and *Atopostipes* of Firmicutes, and *Aequorivita* of Bacteroidetes. *Psychrobacter* is psychrophilic and might help shorten the heating cycle during the composting process, and it has been reported to show a relative abundance of nearly 10% in the initial stage of the bioreactor composting system [63]. In the present study, after SMS addition, the relative abundance of *Psychrobacter* was >30% on day 14, suggesting that *Psychrobacter* may have certain heat resistance ability in the presence of sufficient nitrogen source (SMS). Interestingly, the abundance of *Lactobacillus* (originating from SMS) was higher in SCM and SCMI, accounting for >27% on days 1–5, whereas *Acetobacter* (derived from microbial agent) was not detected.

With the increase in composting temperature, the relative abundance of bacterial genera belonging to branch a gradually decreased, whereas that of the thermophilic bacterial genera belonging to branches b and c increased. In particular, in SCM and SCMI, bacterial genera belonging to branch a could not be detected on day 14. This finding indicated that most of the dominant bacteria associated with the initial raw materials and microbial inoculum could not adapt to the high-temperature composting environment, and that SMS addition could promote the efficient degradation of substrate by high-temperature-tolerant microorganisms. The relative abundance of bacterial genera belonging to branch b, such as the heat-resistant *Saccharomonospora* that can secrete xylanase and lignin peroxidase [64], gradually increased with the composting time and was not affected by SMS addition. In SC, *Thermopolyspora* and *Thermobifida* (belonging to branch c1) became the dominant flora in the middle and late composting stages, and their abundances accounted for >52% on day 14. These two bacterial genera, belonging to the Actinobacteria phylum, have been reported as lignocellulosic degraders and dominant bacterial communities in the cooling and maturation stages of a variety of agricultural and livestock wastes composting processes [14,65]. In contrast, in SCM, the abundance of *Planifilum*, *Novibacillus*, *Bacillus*, and *Geobacillus* belonging to Firmicutes (branch a2) accounted for >42% on day 14. These results were consistent with the phylum-level findings, indicating that SMS addition promoted the growth of spore-forming Firmicutes. However, *Thermopolyspora* and *Thermobifida* became the dominant bacteria in both SCM and SCMI on day 29. In a previous study, [52] found that *Thermopolyspora* and *Thermobifida* were significantly positively correlated with nitrate–nitrogen and TN contents, and they were considered as the possible biomarkers for the maturity stage of composting.

To identify the potential interactions between microbial communities in the composting system, a co-occurrence network between bacteria and fungi were conducted by network analysis (Table S2). In the composition of the interaction, the proportion of bacteria-bacteria interaction is the largest (68.0%), and the correlation is mainly positive.

These positive interactions promoted the degradation of stubborn substances by dominant microorganisms during composting. It is worth noting that although the bacteria–fungi interaction only accounts for 8.5%, its negative correlation (34.9%) is higher than that of bacteria–bacteria (11.34%) and fungi–fungi (3.17%), indicating that there were more drastic competitions between bacteria and fungi for nutrients than those among bacteria and those among fungi [52,66]. Furthermore, there are also positive interactions between bacteria and fungi. The dominant actinobacterium *Thermobifida fusca* and the dominant fungus *Thermomyces lanuginosus* have a synergistic degradation mechanism of lignocellulose in natural corn straw composting [67].

3.5. Metaproteome Analysis of the Dominant Microbial Communities

To further understand the functions of the dominant microbial communities in the four composting systems, active zymography and LTQ-Orbitrap technology were used to identify the changes and sources of the major secreted proteins [14,68]. It must be noted that SMS is a high-nitrogen organic material containing 2% nitrogen (data not shown). The results of gelatin zymography showed that the initial protease bands of SCM and SCMI were significantly brighter than those of SC and SCI (Figure 5a). However, with the increasing composting time, the bands Pro1 and Pro2 of SCM and SCMI gradually became shallower, and the main protease bands became consistent with those of SC and SCI, indicating that the succession of the microbial community led to the functional changes. The number of main bands corresponding to lignocellulose-degrading extracellular enzymes of SCM and SCMI was higher on day 14 and appeared later than the secretion time of SC and SCI (Figure 5b,c), indicating that the addition of high-nitrogen materials such as SMS may lead to the rapid growth of microorganisms that can secrete numerous proteases. The xylanases and endoglucanases activities of all four composts showed an observable rising, which was consistent with the zymogram (Figure S3).

The sequenced proteomes of 21 dominant bacterial genera and seven dominant fungal genera were used as reference database, and the obtained spectral counts were employed to determine the relative abundances of the identified proteins [69]. As shown in Table S1, 25 major lignocellulose-degrading enzymes and 12 major proteases were identified. Five of the functional proteins originated from fungi, among which two cellulases (Q8J0K6 and Q8J0K7) secreted by *Melanocarpus albomyces* were secreted in large quantities after the addition of SMS. The results showed that most of the fungi were less resistant to high temperature, and genomic data showed that fungi were still abundant in the late composting period, which could possibly be due to the derivation of DNA from inactive microorganisms [48]. Bacteria showed stronger degradation function than fungi, and three xylanases (F6LAX2, Q47QL8, and A0A3Q8TLG0), six endoglucanases (Q08166, Q47QG3, P26222, Q9LAV5, Q47MW0, and Q47RH9) and five proteases (Q47L13, Q47M86, Q47R84, Q47SF0, and Q47SP5) from *Thermobifida fusca* were identified, while four xylanases (A0A1I2PGX8, A0A1I2RW64, A0A1I2MI13, A0A1I2N8J0, and A0A2T0LHP9), one endoglucanase (A0A1I2KE01), and five proteases (A0A1I2MW39, A0A1I2SD42, A0A1I2MSC9, A0A1I2KIP3, and A0A1I2RT31) from *Planifilum fulgidum* were detected (Figure 6a), thus signifying that these two genera played a leading role in the degradation of organic matter in the late composting period. Previous studies [14,70] have confirmed that *T. fusca* is the dominant cellulose-degrading bacterium in lignocellulose compost. It has been reported that the abundance of *P. fulgidum* was only 3% in pure chicken manure compost, but it increased to 41% in chicken manure and straw mixed compost [71]. These results suggested that *P. fulgidum* can grow in high-nitrogen substrates such as SMS and chicken manure, and that the presence of both lignocellulose and nitrogen sources can significantly promote bacterial growth. However, further studies are needed to reveal the underlying mechanism of increased *Planifilum* abundance in the presence of carbon and nitrogen sources.

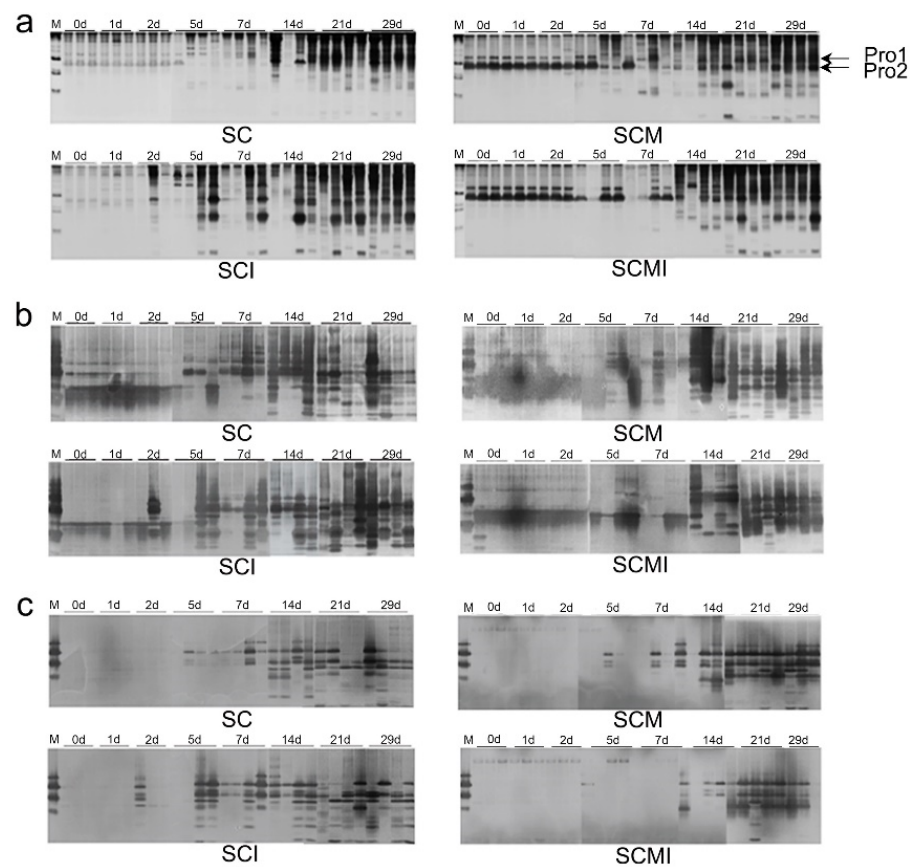


Figure 5. Dynamic changes in proteins and lignocellulose-degrading exoenzymes with time. Zymogram of proteases (a), xylanases (b), and cellobiohydrolases (c).

It can be seen from Figure 6a that the secretion of lignocellulase and protease (especially, protease) was higher in SCM₁₄ and SCMI₁₄ when compared with that in SC₁₄ and SCI₁₄. A heatmap (Figure 6b) of the relative abundances of secreted extracellular proteases in the four composting systems showed that the number of proteins secreted by *Thermobifida* and *Planifilum* was higher during the composting process. The secretion of *P. fulgidum* protease was significantly higher in SCM and SCMI when compared with that in SC and SCI, indicating that the addition of SMS promoted the increase in the secretion of *P. fulgidum* protease (mainly S8, M17, and M32 family protease) (Figure 6c). A possible protein degradation system was mapped by genomic and extracellular proteomics analysis of *P. fulgidum* (Figure S4). It must be noted that the types of proteases secreted by *Thermobifida* and *Planifilum* were different, and there may be a cooperative degradation relationship between these two genera. Furthermore, the analysis of mass spectrometry data revealed that the degradation of proteins in the straw and cow manure mixed with SMS was mainly owing to the synergistic degradation of aminopeptidase and carboxypeptidase secreted by these two dominant bacteria.

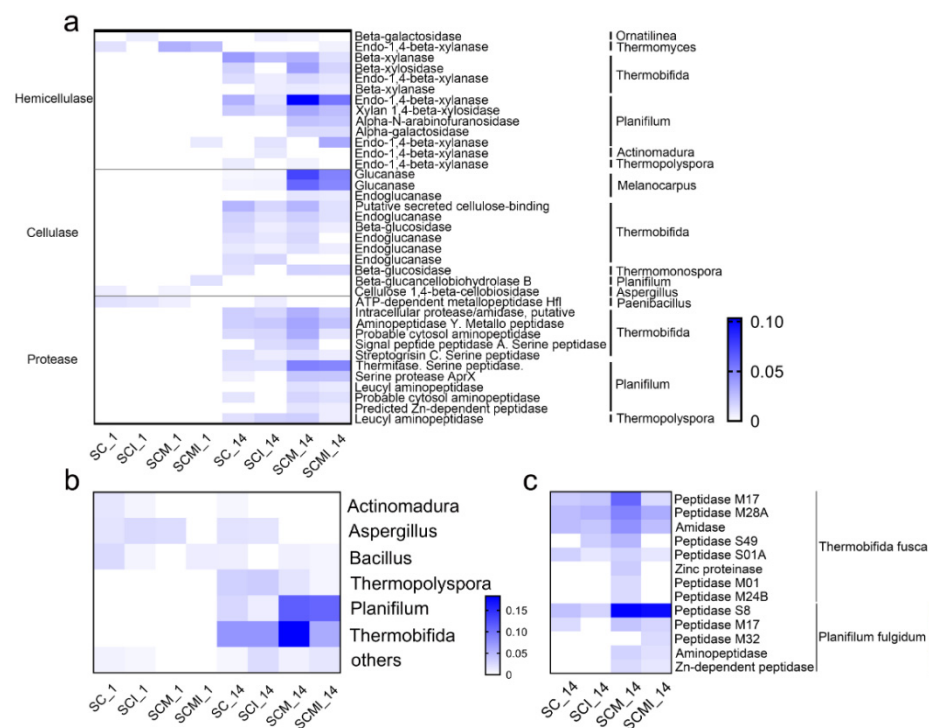


Figure 6. (a) Heatmap of variations types and abundances of extracellular proteins secreted by the dominant genera on day 1 and day 14. (b) Heatmap of protease secreted by the dominant genera on day 1 and day 14. (c) Heatmap of different kinds of peptidase secreted by *T. fusca* and *P. fulgidum* on day 14.

4. Conclusions

In conclusion, the straw and cow manure composted with SMS formed a simple and stable microbial community structure over time, with Ascomycetes, Firmicutes, and Actinomycetes being the dominant microorganisms. The addition of SMS, a high-nitrogen biomass, accelerated the shift from Gram-negative bacteria (Bacteroidetes, Proteobacteria) to Gram-positive bacteria (Firmicutes, Actinomycetes). However, the non-composting dominant bacteria such as *Pichia* and *Lactobacillus* in the microbial agent could not adapt to the high-temperature composting environment and were replaced by thermophilic bacteria after five days of composting. The metaproteomics results indicated that the dominant microorganisms in straw biomass such as *T. fusca* and *P. fulgidum* synergistically degraded hemicellulose, cellulose, and proteins. In particular, *P. fulgidum* was noted to secrete a large number of S8, M17, and M32 family proteases in a high-nitrogen environment to efficiently degrade the high-protein substrates such as SMS. These findings provided a comprehensive understanding of the degradation of SMS co-composting and use of microbial agents, thereby laying a rational foundation for the development of more efficient processes.

Supplementary Materials: The following are available online at <https://www.mdpi.com/article/10.3390/su131810002/s1>, Figure S1: The different genus distributions between the two composts. The difference was considered to be significant between the two data sets at $p < 0.05$ using a t-test analysis, which is indicated by asterisks. a, b, c are bacterial, and e, d, f are fungus. Figure S2. The phylum level composition of the microbiota in four piles. One-way ANOVA analysis was applied on the computation of the abundance changes. Figure S3. The relative xylanase (A) and endoglucanases (B) activities with 1% xylan and CMC as a substrate, respectively. Figure S4. Schematic diagram of *Planifilum fulgidum* protein degradation model predicted based on genomic data and protein mass spectrometry data. Table S1. Functional classified extracellular proteins secreted by the dominant genera in the four groups on day 1 and day 14. Table S2. Composition of edges in the co-occurrence network.

Author Contributions: Conceptualization, H.Z., W.W. and L.W.; methodology, H.Z., Z.L. and C.Y.; data curation, H.Z.; writing—original draft preparation, H.Z.; visualization, L.W.; supervision, S.L.; project administration, L.W.; funding acquisition, W.W. and L.W. All authors have read and agreed to the published version of the manuscript.

Funding: This research was funded by Shandong Provincial Key Research and Development Program (Major Scientific and Technological Innovation Project) (NO.2019JZZY010411); The 2021 first funds for central government to guide local science and technology development in Qinghai Province (No.2021ZY002); Shandong Province Agricultural Major Applied Technology Innovation Project (NO.SD2019ZZ018).

Institutional Review Board Statement: Not applicable.

Informed Consent Statement: Not applicable.

Data Availability Statement: Not applicable.

Conflicts of Interest: The authors declare no conflict of interest.

References

- Zhu, H.J.; Sun, L.F.; Zhang, Y.F.; Zhang, X.L.; Qiao, J.J. Conversion of spent mushroom substrate to biofertilizer using a stress-tolerant phosphate-solubilizing *Pichia. farinose*. FL7. *Bioresour. Technol.* **2012**, *111*, 410–416. [[CrossRef](#)]
- Finney, K.N.; Ryu, C.; Sharifi, V.N.; Swithenbank, J. The reuse of spent mushroom compost and coal tailings for energy recovery: Comparison of thermal treatment technologies. *Bioresour. Technol.* **2009**, *100*, 310–315. [[CrossRef](#)] [[PubMed](#)]
- Hu, T.; Wang, X.; Zhen, L.; Gu, J.; Zhang, K.; Wang, Q.; Ma, J.; Peng, H.; Lei, L.; Zhao, W. Effects of inoculating with lignocellulose-degrading consortium on cellulose-degrading genes and fungal community during co-composting of spent mushroom substrate with swine manure. *Bioresour. Technol.* **2019**, *291*, 121876. [[CrossRef](#)] [[PubMed](#)]
- Huang, J.L.; Liu, J.Y.; Chen, J.C.; Xie, W.M.; Kuo, J.H.; Lu, X.W.; Chang, K.L.; Wen, S.T.; Sun, G.; Cai, H.M. Combustion behaviors of spent mushroom substrate using TG-MS and TG-FTIR: Thermal conversion, kinetic, thermodynamic and emission analyses. *Bioresour. Technol.* **2018**, *266*, 389–397. [[CrossRef](#)]
- Fang, W.; Zhang, P.Y.; Gou, X.Y.; Zhang, H.B.; Wu, Y.; Ye, J.; Zeng, G.M. Volatile fatty acid production from spent mushroom compost: Effect of total solid content. *Int. Biodeterior Biodegrad.* **2016**, *113*, 217–221. [[CrossRef](#)]
- Lou, Z.M.; Zhu, J.; Wang, Z.X.; Baig, S.A.; Fang, L.; Hu, B.L.; Xu, X.H. Release characteristics and control of nitrogen, phosphate, organic matter from spent mushroom compost amended soil in a column experiment. *Process. Saf. Environ. Prot.* **2015**, *98*, 417–423. [[CrossRef](#)]
- Duan, Y.; Awasthi, S.K.; Liu, T.; Verma, S.; Wang, Q.; Chen, H.; Ren, X.; Zhang, Z.; Awasthi, M.K. Positive impact of biochar alone and combined with bacterial consortium amendment on improvement of bacterial community during cow manure composting. *Bioresour. Technol.* **2019**, *280*, 79–87. [[CrossRef](#)] [[PubMed](#)]
- Wan, L.; Wang, X.; Cong, C.; Li, J.; Xu, Y.; Li, X.; Hou, F.; Wu, Y.; Wang, L. Effect of inoculating microorganisms in chicken manure composting with maize straw. *Bioresour. Technol.* **2020**, *301*, 122730. [[CrossRef](#)]
- Ren, G.M.; Xu, X.H.; Qu, J.J.; Zhu, L.P.; Wang, T.T. Evaluation of microbial population dynamics in the co-composting of cow manure and rice straw using high throughput sequencing analysis. *World J. Microb. Biot.* **2016**, *32*, 1–11. [[CrossRef](#)]
- Wang, R.; Zhang, J.; Sui, Q.; Wan, H.; Tong, J.; Chen, M.; Wei, Y.; Wei, D. Effect of red mud addition on tetracycline and copper resistance genes and microbial community during the full scale swine manure composting. *Bioresour. Technol.* **2016**, *216*, 1049–1057. [[CrossRef](#)]
- Meng, L.; Li, W.; Zhang, S.; Wu, C.; Lv, L. Feasibility of co-composting of sewage sludge, spent mushroom substrate and wheat straw. *Bioresour. Technol.* **2017**, *226*, 39–45. [[CrossRef](#)] [[PubMed](#)]
- Das, M.; Uppal, H.S.; Singh, R.; Beri, S.; Mohan, K.S.; Gupta, V.C.; Adholeya, A. Co-composting of physic nut (*Jatropha curcas*) deoiled cake with rice straw and different animal dung. *Bioresour. Technol.* **2011**, *102*, 6541–6546. [[CrossRef](#)] [[PubMed](#)]
- Paredes, C.; Bernal, M.P.; Cegarra, J.; Roig, A. Bio-degradation of olive mill wastewater sludge by its co-composting with agricultural wastes. *Bioresour. Technol.* **2002**, *85*, 1–8. [[CrossRef](#)]
- Zhang, L.L.; Ma, H.X.; Zhang, H.Q.; Xun, L.Y.; Chen, G.J.; Wang, L.S. *Thermomyces lanuginosus* is the dominant fungus in maize straw composts. *Bioresour. Technol.* **2015**, *197*, 266–275. [[CrossRef](#)]
- Fendrihan, S.; Pop, C.E. Biotechnological potential of plant associated microorganisms. *Rom. Biotechnol. Lett.* **2021**, *26*, 2700–2706. [[CrossRef](#)]
- Lyu, D.; Backer, R.; Subramanian, S.; Smith, D.L. Phytomicrobiome Coordination Signals Hold Potential for Climate Change-Resilient Agriculture. *Front. Plant. Sci.* **2020**, *11*, 634. [[CrossRef](#)] [[PubMed](#)]
- Shubina, V.; Birsu, M.; Burtseva, S. Antifungal Activity of Bacteria of the Genus *Bacillus* and *Streptomyces* isolated from the Soil of the Republic of Moldova. *Mikrobiolohichniy Zhurnal* **2018**, *80*, 41–53. [[CrossRef](#)]
- Wang, N.; Wang, L.; Zhu, K.; Hou, S.; Chen, L.; Mi, D.; Gui, Y.; Qi, Y.; Jiang, C.; Guo, J.H. Plant Root Exudates Are Involved in *Bacillus cereus* AR156 Mediated Biocontrol Against *Ralstonia solanacearum*. *Front. Microbiol.* **2019**, *10*, 98. [[CrossRef](#)]

19. Meng, X.; Liu, B.; Xi, C.; Luo, X.; Yuan, X.; Wang, X.; Zhu, W.; Wang, H.; Cui, Z. Effect of pig manure on the chemical composition and microbial diversity during co-composting with spent mushroom substrate and rice husks. *Bioresour. Technol.* **2018**, *251*, 22–30. [[CrossRef](#)]
20. Wu, D.; Wei, Z.; Gao, X.; Wu, J.; Chen, X.; Zhao, Y.; Jia, L.; Wen, D. Reconstruction of core microbes based on producing lignocellulolytic enzymes causing by bacterial inoculation during rice straw composting. *Bioresour. Technol.* **2020**, *315*, 123849. [[CrossRef](#)]
21. Xiao, Z.; Lin, M.H.; Fan, J.L.; Chen, Y.X.; Zhao, C.; Liu, B. Anaerobic digestion of spent mushroom substrate under thermophilic conditions: Performance and microbial community analysis. *Appl. Microbiol. Biot.* **2018**, *102*, 499–507. [[CrossRef](#)]
22. Zhang, L.; Zhang, H.; Wang, Z.; Chen, G.; Wang, L. Dynamic changes of the dominant functioning microbial community in the compost of a 90-m³ aerobic solid state fermentor revealed by integrated meta-omics. *Bioresour. Technol.* **2016**, *203*, 1–10. [[CrossRef](#)]
23. Chi, C.P.; Chu, S.; Wang, B.; Zhang, D.; Zhi, Y.; Yang, X.; Zhou, P. Dynamic bacterial assembly driven by *Streptomyces. griseorubens*. JSD-1 inoculants correspond to composting performance in swine manure and rice straw co-composting. *Bioresour. Technol.* **2020**, *313*, 123692. [[CrossRef](#)]
24. Yang, X.; Hu, Q.; Han, Z.; Ruan, X.; Jiang, S.; Chai, J.; Zheng, R. Effects of exogenous microbial inoculum on the structure and dynamics of bacterial communities in swine carcass composting. *Can. J. Microbiol.* **2018**, *64*, 1042–1053. [[CrossRef](#)]
25. Wei, Y.; Wu, D.; Wei, D.; Zhao, Y.; Wu, J.; Xie, X.; Zhang, R.; Wei, Z. Improved lignocellulose-degrading performance during straw composting from diverse sources with actinomycetes inoculation by regulating the key enzyme activities. *Bioresour. Technol.* **2019**, *271*, 66–74. [[CrossRef](#)] [[PubMed](#)]
26. Mao, H.; Lv, Z.; Sun, H.; Li, R.; Zhai, B.; Wang, Z.; Awasthi, M.K.; Wang, Q.; Zhou, L. Improvement of biochar and bacterial powder addition on gaseous emission and bacterial community in pig manure compost. *Bioresour. Technol.* **2018**, *258*, 195–202. [[CrossRef](#)] [[PubMed](#)]
27. Zhang, Y.; Zhao, Y.; Chen, Y.; Lu, Q.; Li, M.; Wang, X.; Wei, Y.; Xie, X.; Wei, Z. A regulating method for reducing nitrogen loss based on enriched ammonia-oxidizing bacteria during composting. *Bioresour. Technol.* **2016**, *221*, 276–283. [[CrossRef](#)]
28. Zhao, Y.; Li, W.; Chen, L.; Meng, L.; Zheng, Z. Effect of enriched thermotolerant nitrifying bacteria inoculation on reducing nitrogen loss during sewage sludge composting. *Bioresour. Technol.* **2020**, *311*, 123461. [[CrossRef](#)] [[PubMed](#)]
29. Jiang, J.; Liu, X.; Huang, Y.; Huang, H. Inoculation with nitrogen turnover bacterial agent appropriately increasing nitrogen and promoting maturity in pig manure composting. *Waste Manag.* **2015**, *39*, 78–85. [[CrossRef](#)] [[PubMed](#)]
30. Ballardo, C.; Vargas-Garcia, M.D.C.; Sanchez, A.; Barrena, R.; Artola, A. Adding value to home compost: Biopesticide properties through *Bacillus. thuringiensis*. inoculation. *Waste Manag.* **2020**, *106*, 32–43. [[CrossRef](#)] [[PubMed](#)]
31. Ahn, H.K.; Richard, T.L.; Glanville, T.D. Laboratory determination of compost physical parameters for modeling of airflow characteristics. *Waste Manag.* **2008**, *28*, 660–670. [[CrossRef](#)] [[PubMed](#)]
32. Kwaansa-Ansah, E.E.; Voegborlo, R.B.; Adimado, A.A.; Ephraim, J.H.; Nriagu, J.O. Effect of pH, sulphate concentration and total organic carbon on mercury accumulation in sediments in the Volta Lake at Yeji, Ghana. *Bull. Environ. Contam. Toxicol.* **2012**, *88*, 418–421. [[CrossRef](#)] [[PubMed](#)]
33. Zhang, L.; Sun, X. Changes in physical, chemical, and microbiological properties during the two-stage co-composting of green waste with spent mushroom compost and biochar. *Bioresour. Technol.* **2014**, *171*, 274–284. [[CrossRef](#)]
34. Xing, S.; Li, G.; Sun, X.; Ma, S.; Chen, G.; Wang, L.; Gao, P. Dynamic changes in xylanases and beta-1,4-endoglucanases secreted by *Aspergillus. niger*. An-76 in response to hydrolysates of lignocellulose polysaccharide. *Appl. Biochem. Biotechnol.* **2013**, *171*, 832–846. [[CrossRef](#)]
35. Zhang, X.; Liu, N.; Yang, F.; Li, J.; Wang, L.; Chen, G.; Gao, P. In situ demonstration and quantitative analysis of the intrinsic properties of glycoside hydrolases. *Electrophoresis* **2012**, *33*, 280–287. [[CrossRef](#)] [[PubMed](#)]
36. Tsujii, M.; Kawano, S.; DuBois, R.N. Cyclooxygenase-2 expression in human colon cancer cells increases metastatic potential. *Proc. Natl. Acad. Sci. USA* **1997**, *94*, 3336–3340. [[CrossRef](#)]
37. Magoc, T.; Salzberg, S.L. FLASH: Fast length adjustment of short reads to improve genome assemblies. *Bioinformatics* **2011**, *27*, 2957–2963. [[CrossRef](#)] [[PubMed](#)]
38. Edgar, R.C. UPARSE: Highly accurate OTU sequences from microbial amplicon reads. *Nat. Methods* **2013**, *10*, 996–998. [[CrossRef](#)]
39. Wang, Q.; Garrity, G.M.; Tiedje, J.M.; Cole, J.R. Naive Bayesian classifier for rapid assignment of rRNA sequences into the new bacterial taxonomy. *Appl. Environ. Microbiol.* **2007**, *73*, 5261–5267. [[CrossRef](#)]
40. Zhang, L.L.; Li, L.J.; Sha, G.M.; Liu, C.X.; Wang, Z.H.; Wang, L.S. Aerobic composting as an effective cow manure management strategy for reducing the dissemination of antibiotic resistance genes: An integrated meta-omics study. *J. Hazard. Mater.* **2020**, 386. [[CrossRef](#)]
41. Bradford, M.M. A rapid and sensitive method for the quantitation of microgram quantities of protein utilizing the principle of protein-dye binding. *Anal. Biochem.* **1976**, *72*, 248–254. [[CrossRef](#)]
42. Zhang, L.; Sun, X.Y.; Tian, Y.; Gong, X.Q. Effects of brown sugar and calcium superphosphate on the secondary fermentation of green waste. *Bioresour. Technol.* **2013**, *131*, 68–75. [[CrossRef](#)] [[PubMed](#)]
43. Wu, Y.P.; Chen, Y.X.; Shaaban, M.; Zhu, D.W.; Hu, C.X.; Chen, Z.B.; Wang, Y. Evaluation of microbial inoculants pretreatment in straw and manure co-composting process enhancement. *J. Clean. Prod.* **2019**, *239*, 118078. [[CrossRef](#)]

44. Xie, X.Y.; Zhao, Y.; Sun, Q.H.; Wang, X.Q.; Cui, H.Y.; Zhang, X.; Li, Y.J.; Wei, Z.M. A novel method for contributing to composting start-up at low temperature by inoculating cold-adapted microbial consortium. *Bioresour. Technol.* **2017**, *238*, 39–47. [[CrossRef](#)]
45. Li, S.Y.; Li, D.Y.; Li, J.J.; Li, Y.Y.; Li, G.X.; Zang, B.; Li, Y. Effect of spent mushroom substrate as a bulking agent on gaseous emissions and compost quality during pig manure composting. *Environ. Sci. Pollut. R.* **2018**, *25*, 12398–12406. [[CrossRef](#)]
46. Gong, X.; Li, S.; Carson, M.A.; Chang, S.X.; Wu, Q.; Wang, L.; An, Z.; Sun, X. Spent mushroom substrate and cattle manure amendments enhance the transformation of garden waste into vermicomposts using the earthworm *Eisenia fetida*. *J. Environ. Manag.* **2019**, *248*, 109263. [[CrossRef](#)]
47. Hanc, A.; Chadimova, Z. Nutrient recovery from apple pomace waste by vermicomposting technology. *Bioresour. Technol.* **2014**, *168*, 240–244. [[CrossRef](#)]
48. Zhang, L.; Sun, X. Influence of bulking agents on physical, chemical, and microbiological properties during the two-stage composting of green waste. *Waste Manag.* **2016**, *48*, 115–126. [[CrossRef](#)]
49. Perez-Godinez, E.A.; Lagunes-Zarate, J.; Corona-Hernandez, J.; Barajas-Aceves, M. Growth and reproductive potential of *Eisenia foetida*. (Sav) on various zoo animal dung after two methods of pre-composting followed by vermicomposting. *Waste Manag.* **2017**, *64*, 67–78. [[CrossRef](#)] [[PubMed](#)]
50. Lasaridi, K.; Protopapa, I.; Kotsou, M.; Pilidis, G.; Manios, T.; Kyriacou, A. Quality assessment of composts in the Greek market: The need for standards and quality assurance. *J. Environ. Manage.* **2006**, *80*, 58–65. [[CrossRef](#)] [[PubMed](#)]
51. Zhu, P.C.; Li, Y.C.; Gao, Y.F.; Yin, M.Q.; Wu, Y.X.; Liu, L.L.; Du, N.; Liu, J.; Yu, X.N.; Wang, L.S. Insight into the effect of nitrogen-rich substrates on the community structure and the co-occurrence network of thermophiles during lignocellulose-based composting. *Bioresour. Technol.* **2021**, *319*. [[CrossRef](#)]
52. Bello, A.; Han, Y.; Zhu, H.; Deng, L.; Yang, W.; Meng, Q.; Sun, Y.; Egbeagu, U.U.; Sheng, S.; Wu, X. Microbial community composition, co-occurrence network pattern and nitrogen transformation genera response to biochar addition in cattle manure-maize straw composting. *Sci. Total Environ.* **2020**, *721*, 137759. [[CrossRef](#)]
53. Zhang, J.; Zeng, G.; Chen, Y.; Yu, M.; Yu, Z.; Li, H.; Yu, Y.; Huang, H. Effects of physico-chemical parameters on the bacterial and fungal communities during agricultural waste composting. *Bioresour. Technol.* **2011**, *102*, 2950–2956. [[CrossRef](#)] [[PubMed](#)]
54. Steger, K.; Jarvis, A.; Vasara, T.; Romantschuk, M.; Sundh, I. Effects of differing temperature management on development of Actinobacteria populations during composting. *Res. Microbiol.* **2007**, *158*, 617–624. [[CrossRef](#)]
55. Nakasaki, K.; Hirai, H. Temperature control strategy to enhance the activity of yeast inoculated into compost raw material for accelerated composting. *Waste Manag.* **2017**, *65*, 29–36. [[CrossRef](#)] [[PubMed](#)]
56. Neher, D.A.; Weicht, T.R.; Bates, S.T.; Leff, J.W.; Fierer, N. Changes in bacterial and fungal communities across compost recipes, preparation methods, and composting times. *PLoS. ONE* **2013**, *8*, e79512.
57. Jiang, X.; Deng, L.; Meng, Q.; Sun, Y.; Han, Y.; Wu, X.; Sheng, S.; Zhu, H.; Ayodeji, B.; Egbeagu, U.U. Fungal community succession under influence of biochar in cow manure composting. *Environ. Sci. Pollut. Res. Int.* **2020**, *27*, 9658–9668. [[CrossRef](#)]
58. Tian, X.; Yang, T.; He, J.; Chu, Q.; Jia, X.; Huang, J. Fungal community and cellulose-degrading genes in the composting process of Chinese medicinal herbal residues. *Bioresour. Technol.* **2017**, *241*, 374–383. [[CrossRef](#)] [[PubMed](#)]
59. Wang, K.; Yin, X.; Mao, H.; Chu, C.; Tian, Y. Changes in structure and function of fungal community in cow manure composting. *Bioresour. Technol.* **2018**, *255*, 123–130. [[CrossRef](#)] [[PubMed](#)]
60. Narang, S.; Sahai, V.; Bisaria, V.S. Optimization of xylanase production by *Melanocarpus albomyces* IIS68 in solid state fermentation using response surface methodology. *J. Biosci. Bioeng.* **2001**, *91*, 425–427. [[CrossRef](#)]
61. Li, P.; Liu, M.; Ma, X.; Wu, M.; Jiang, C.; Liu, K.; Liu, J.; Li, Z. Responses of microbial communities to a gradient of pig manure amendment in red paddy soils. *Sci. Total Environ.* **2020**, *705*, 135884. [[CrossRef](#)] [[PubMed](#)]
62. Meng, Q.; Xu, X.; Zhang, W.; Men, M.; Xu, B.; Deng, L.; Bello, A.; Jiang, X.; Sheng, S.; Wu, X. Bacterial community succession in dairy manure composting with a static composting technique. *Can. J. Microbiol.* **2019**, *65*, 436–449. [[CrossRef](#)] [[PubMed](#)]
63. Ding, J.; Wei, D.; An, Z.; Zhang, C.; Jin, L.; Wang, L.; Li, Y.; Li, Q. Succession of the bacterial community structure and functional prediction in two composting systems viewed through metatranscriptomics. *Bioresour. Technol.* **2020**, *313*, 123688. [[CrossRef](#)] [[PubMed](#)]
64. Zhang, Y.; Pu, J.W.; Liu, X.M.; Wu, Y.Y. Characterization of the alkali-tolerant thermostable enzyme from *Saccharomonospora Viridis* and its application in pulp bleaching. *Cell. Chem. Technol.* **2008**, *42*, 363–369.
65. Storey, S.; Chualain, D.N.; Doyle, O.; Clipson, N.; Doyle, E. Comparison of bacterial succession in green waste composts amended with inorganic fertiliser and wastewater treatment plant sludge. *Bioresour. Technol.* **2015**, *179*, 71–77. [[CrossRef](#)]
66. Zhu, P.; Qin, H.; Zhang, H.; Luo, Y.; Ru, Y.; Li, J.; San, K.W.; Wang, L.; Yu, X.; Guo, W. Variations in antibiotic resistance genes and removal mechanisms induced by C/N ratio of substrate during composting. *Sci. Total Environ.* **2021**, *798*, 149288. [[CrossRef](#)]
67. Shi, Z.; Han, C.; Zhang, X.; Tian, L.; Wang, L. Novel Synergistic Mechanism for Lignocellulose Degradation by a Thermophilic Filamentous Fungus and a Thermophilic Actinobacterium Based on Functional Proteomics. *Front. Microbiol.* **2020**, *11*, 539438. [[CrossRef](#)]
68. Makarov, A.; Denisov, E.; Lange, O.; Horning, S. Dynamic range of mass accuracy in LTQ Orbitrap hybrid mass spectrometer. *J. Am. Soc. Mass Spectrom.* **2006**, *17*, 977–982. [[CrossRef](#)]
69. Saykhedkar, S.; Ray, A.; Ayoubi-Canaan, P.; Hartson, S.D.; Prade, R.; Mort, A.J. A time course analysis of the extracellular proteome of *Aspergillus nidulans* growing on sorghum stover. *Biotechnol. Biofuels* **2012**, *5*, 52. [[CrossRef](#)]

-
70. Wilson, D.B. Studies of *Thermobifida fusca* plant cell wall degrading enzymes. *Chem. Rec.* **2004**, *4*, 72–82. [[CrossRef](#)]
 71. Zhang, L.; Li, L.; Pan, X.; Shi, Z.; Feng, X.; Gong, B.; Li, J.; Wang, L. Enhanced Growth and Activities of the Dominant Functional Microbiota of Chicken Manure Composts in the Presence of Maize Straw. *Front. Microbiol.* **2018**, *9*, 1131. [[CrossRef](#)] [[PubMed](#)]